NATIONAL ADVISORY COMMITTEE FOR AERONAUTICS

TECHNICAL NOTE 3522

MEASUREMENTS OF THE EFFECTS OF FINITE SPAN ON THE

PRESSURE DISTRIBUTION OVER DOUBLE-WEDGE WINGS

AT MACH NUMBERS NEAR SHOCK ATTACHMENT

By Walter G. Vincenti

Ames Aeronautical Laboratory
Moffett Field, Calif.

NACA

Washington
September 1955

NATIONAL ADVISORY COMMITTEE FOR AERONAUTICS

TECHNICAL NOTE 3522

MEASUREMENTS OF THE EFFECTS OF FINITE SPAN ON THE

PRESSURE DISTRIBUTION OVER DOUBLE-WEDGE WINGS

AT MACH NUMBERS NEAR SHOCK ATTACHMENT

By Walter G. Vincenti

SUMMARY

Results are presented of wind-tunnel measurements of the pressure
distribution at low supersonic speeds on two rectangular wings of double-
wedge section and aspect ratios 2 and 4. Comparable results for aspect
ratio infinity have been published in NACA TN 3225. As in the previous
work the data cover the Mach number range from 1.166 to 1.377, which
brackets the value of 1.221 given by exact inviscid theory for attachment
of the shock wave to the leading edge at zero angle of attack. The angle-
of-attack range is from 0° to 5° and the Reynolds number is 0.54 million.
The data are discussed in detail and compared with the previous two-
dimensional findings.

The pressure-drag coefficient at zero lift is found to decrease with
decrease in aspect ratio at all values of the test Mach number. This
effect is most pronounced at Mach numbers at which the shock wave is
detached. As a result, the rise in drag coefficient with decreasing Mach
number, which was fairly pronounced in the two-dimensional case, becomes
less evident as the aspect ratio is reduced. The reasons for this behavior
are apparent in the pressure distributions.

As would be expected, decreasing the aspect ratio decreases the rise
of lift with angle of attack. This effect grows rapidly as the shock wave
becomes detached. Decreasing the aspect ratio also decreases the non-
linearity of the lift curve at Mach numbers near shock detachment. Because
of this, the local peak of initial lift-curve slope as a function of Mach
number, evident in this vicinity in the two-dimensional case, is absent
at aspect ratio 2.

The drag due to angle of attack is affected by a variation of chord
force as well as normal force. On the front wedge in the two-dimensional
case, the increment in chord force (as measured from the chord force at
zero lift) changes from positive to negative as the Mach number decreases
past detachment. Reducing the aspect ratio reduces the magnitude of this

change. The net result as regards the drag due to angle of attack is that the effect of aspect ratio is now greatest at Mach numbers just above detachment and diminishes with Mach number change in either direction.

Theoretical considerations also lead to certain conclusions regarding wave detachment. In particular, detachment of the shock wave from a wedge of finite span can be shown to occur at the same free-stream Mach number as from a wedge of infinite span. The detachment will occur simultaneously at all points across the span (except possibly the tips). At Mach numbers below detachment the sonic speed at zero angle of attack need not be attained at the ridge as in the two-dimensional case but may occur forward on the face of the wedge. This fact is confirmed by the experiments.

INTRODUCTION

The aerodynamic properties of wedges of infinite span at Mach numbers near shock attachment have now been well explored. For the zero-lift case, theoretical studies have been made on the basis of the transonic (i.e., nonlinear) small-disturbance theory by Guderley (ref. 1) and Vincenti and Wagoner (ref. 2). The quantitative results of the latter reference have been compared with experiment by Liepmann and Bryson (refs. 3 and 4) and Griffith (ref. 5). Good agreement was observed for wedges up to the thickest studied (total angle of 20°).[1] For the lifting wedge, theoretical calculations have been made by Guderley and Yoshihara (ref. 8), Vincenti and Wagoner (ref. 9), and Yoshihara (ref. 10). These calculations brought to light the interesting fact that the lift-curve slope at zero lift has a pronounced maximum at or near the attachment Mach number. This finding has since been confirmed by the experimental work of reference 11.

Information on wedges of finite span is less extensive. Since three-dimensional problems are as yet beyond the reach of transonic theory, knowledge here must come from experiment. Existing work in this regard is limited apparently to two reports, one by Orman, Rae, and Ward (ref. 12) and the other by Hilton (ref. 13). The first of these gives the results of chordwise and spanwise pressure-distribution measurements on four double-wedge wings of various aspect ratios (maximum 1.5) at three supersonic Mach numbers. All of the Mach numbers gave an attached wave at zero angle of attack, but two were low enough that the wave presumably was detached at the higher angles. The paper by Hilton presents chordwise pressure data at the midspan of a single wedge of aspect ratio 3.3. The data are for one Mach number only; again the wave is attached at zero angle but becomes detached as the angle is increased.

---

[1]Reference should also be made to a note by Spreiter (ref. 6), who has re-examined the data of Liepmann and Bryson in the light of more recent developments. For the correction of an error in this note, see also reference 7.

   The present report contains data obtained by extension of the work
of reference 11. In this earlier investigation essentially two-dimensional
results for a double-wedge section of approximately 8-percent thickness
were obtained by measurements of pressure at midspan on a wing of aspect
ratio 9.6. The Mach number range of the tests was from 1.166 to 1.377.
This brackets the value of 1.221 given by exact inviscid theory for attach-
ment of the bow wave at zero angle of attack. The present report provides
data obtained from pressure-distribution measurements over the plan form
of two additional wings of aspect ratio 4 and 2. The data cover the same
Mach number range as before. As in the earlier work, the angle of attack
varies from 0 to somewhat less than 5°. Discussion of the data is carried
out in the light of the previous two-dimensional findings.

NOTATION

Primary Symbols

A aspect ratio

$\tilde{A}$ $\left[(\gamma + 1)M_\infty^2(t/c) \right]^{1/3} A$

b wing span

c wing chord

c_d section pressure-drag coefficient, $\dfrac{\text{pressure drag per unit span}}{q_\infty c}$

c_l section lift coefficient, $\dfrac{\text{lift per unit span}}{q_\infty c}$

C_C chord-force coefficient, $\dfrac{\text{chord force}}{q_\infty cb}$

C_D pressure-drag coefficient, $\dfrac{\text{pressure drag}}{q_\infty cb}$

$\tilde{C}_D$ $\left[(\gamma + 1)M_\infty^2 \right]^{1/3} C_D/(t/c)^{5/3}$

C_L lift coefficient, $\dfrac{\text{lift}}{q_\infty cb}$

$\widetilde{C_L/\alpha}$ $\left[(\gamma + 1)M_\infty^2(t/c) \right]^{1/3} C_L/\alpha$

C_p pressure coefficient, $\dfrac{p-p_\infty}{q_\infty}$

M   Mach number

p   static pressure

Δp   difference in static pressure between bottom and top of wing

q   dynamic pressure

t   maximum thickness of wing section

x   chordwise distance from leading edge, positive rearward

$\bar{x}$ chordwise distance from leading edge to center of lift, positive
         rearward

y   spanwise distance from midspan, positive to right for observer
         looking upstream

α angle of attack

γ ratio of specific heats (7/5 for air)

θ_w half angle of wedge

ξ_∞ transonic similarity parameter, $\dfrac{M_\infty^2 - 1}{\left[(\gamma + 1) M_\infty^2 (t/c) \right]^{2/3}}$

Subscripts

∞ free-stream conditions

f   value for front wedge

r   value for rear wedge

o   value at $\alpha = 0$

APPARATUS AND TEST METHODS

The investigation was performed in the Ames 6- by 6-foot supersonic wind tunnel. The experimental procedure was identical with that of reference 11, except for the matters described in the following paragraphs.

Models

The models for the present tests are shown in figures 1 and 2. The aspect-ratio-9.6 wing of reference 11 is included for comparison. In all cases the wing section was a doubly symmetrical double wedge with an included angle of 9° at the leading and trailing edges (corresponding to a thickness ratio of 0.0787). As explained in reference 11, the wing of the earlier investigation was made entirely of tool steel. Here, because of the increased number of orifices, the construction was of bismuth-tin alloy cast over a steel plate. Stainless-steel tubes, which were used for the pressure leads, were installed in the plate prior to casting. The ends of the tubes were made originally to extend up through the alloy, so that the tubes themselves became the pressure orifices upon final machining of the surface. The leading and trailing edges of the wings were made of brass strips inserted into the basic steel plate before the alloy was applied. Brass was used here to assure an adequate bond at the feather edge that exists where the alloy tapers to an end on the brass. After casting, the bismuth-tin alloy, brass strips, and stainless-steel tubes were machined and polished as a unit to obtain the final surface of the wing. As in reference 11, the final thickness of the leading edge was 0.003 inch.

The measuring orifices of the present wings were placed in the top surface over one-half the span. The aspect-ratio-4 wing had 85 orifices at 6 spanwise stations; the aspect-ratio-2 wing, 76 orifices at 5 spanwise stations. Besides these primary orifices, each of the wings had two secondary orifices on the bottom surface at midspan. These orifices provided a check on the angle of attack as explained in reference 11. The orifice diameter on the present wings was 0.030 inch as against 0.018 inch on the wing of reference 11.

The support for all the wings was provided by a rearward sting as described in reference 11. As shown in figures 1 and 2, this sting was offset so that it joined the wing a small distance from the center line on the half of the span not containing the orifices. As explained in reference 11, this distance was chosen such that, at the supersonic speeds anticipated on the rear of the wing, the orifices would all lie outside the theoretical region of influence (viscous effects neglected) of the forwardmost part of the sting. A study of the measured pressure distributions at the various spanwise stations indicates that the effect was indeed negligible, except possibly on the high-pressure side of the rear wedge at the highest angles of attack. The auxiliary wires that were needed to support the wing tips in reference 11 were not required here because of the reduced span of the wings.

Reduction of Data

Reduction of the test data was carried out in the general manner
described in reference 11. The primary difference was that it was
necessary in the present case to make a spanwise integration to find the
over-all force and moment coefficients. This was done by plotting the
section coefficients as functions of y/b and integrating mechanically.
Because of the additional integration, the over-all coefficients are likely
to be less accurate than the two-dimensional values of the previous work.

As explained in reference 11, the final results for a given angle of
attack were arrived at in every case by combining data for equal positive
and negative settings of the wing. This was necessary because of the
restriction of the pressure orifices to one surface of the model. After
tests of the aspect-ratio-4 wing were completed, however, it was found
that the reference from which the angular settings of this wing were
measured had been misset by 0.15°. As a result, supposedly equal positive
and negative angles were not the same but differed by 0.30°. To correct
for this error, data for this wing were plotted as a function of angle
of attack, and the values for equal positive and negative angles read
from the resulting curves. All results shown for the aspect-ratio-4 wing
were obtained in this manner. There are also indications that the tests
of this wing, which were run last, were accompanied by larger and more
erratic backlash in the angle mechanism than was present for the other
wings (cf. ref. 11, p. 6). For this reason the angles of attack for A = 4
may be less reliable than for the other wings, even after the above
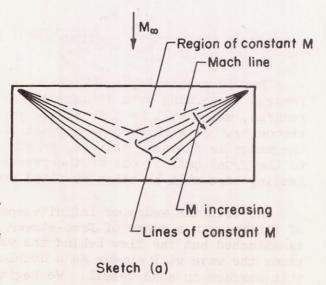correction.

PRELIMINARY REMARKS

Before proceeding to the results, it may be well to set down a few
remarks concerning wave detachment for a wedge of finite span. These
remarks, which will be theoretical in nature, will assume a fluid of zero
viscosity. It will also be assumed that the chord as well as the span of
the wedge is finite - that is, we concern ourselves with an object similar
to the front half of one of the present wings. The included angle at the
leading edge will be taken as fixed and the angle of attack as zero.[2]

As with the wedge of infinite span, there will exist for the wedge
of finite span a range of free-stream Mach number in which the shock wave
is attached but the flow behind the wave is subsonic. Under these condi-
tions the wave will appear as a double-curved surface. Let us examine
this surface in some detail. We begin by recalling the general fact,

_____

[2]The corresponding phenomena for a wedge of infinite span are
described in general terms in reference 2 and in detail in references 1
and 14.

known from oblique-shock theory, that for a given value of the free-stream
Mach number M_∞ the wave angle at any point and the corresponding condi-
tions on the downstream side of the wave are determined uniquely if the
deflection of the flow through the wave is known.[3] This is true provided
the wave and deflection angles are measured in the plane that contains
the free-stream velocity vector and the normal to the shock wave at the
point in question. Now let us apply these considerations to the flow at
the leading edge itself. Here, because the wave must be attached to the
straight edge, the plane containing the free-stream vector and the normal
to the wave must (even if the wave is twisted) be normal to the edge at
every point along the span. The pertinent deflection angle at points on
the leading edge is thus the leading-edge angle itself, which is constant
across the span. It follows that, as long as the shock wave is attached,
the wave angle and the flow quantities directly at the leading edge must
likewise be constant across the span. This is true even though the flow
downstream of the wave is subsonic (and hence generally nonuniform). The
magnitude of the various quantities at the leading edge will obviously be
the same as on a wedge of infinite span at the same value of M_∞. This
means that sonic speed will occur at the leading edge at the same free-
stream Mach number as in the two-dimensional case, and - most important -
that the shock wave will detach from a wedge of finite span at the same
value of M_∞ as from a wedge of infinite span. By the same token, the
detachment will occur simultaneously at all points across the span (except
possibly at the tips). These results must hold no matter how small the
aspect ratio of the wedge - that is, the aerodynamic behavior of a wedge
does not approach that of a pointed object such as a cone as the aspect
ratio tends to zero. This is a consequence of the finite length of leading
edge always present on the wedge.

A few remarks can also be
made about the flow on the wedge
aft of the shock wave. It is
apparent, for example, that at a
value of M_∞ sufficiently above
detachment, the effects of finite
span must be confined to regions
bounded by the Mach lines from
the forwardmost point of each tip
(sketch (a)). Between these Mach
lines and the leading edge there
will exist a region of triangular
shape in which the local Mach num-
ber M is constant at a super-
sonic value less than M_∞. To the
rear of the Mach lines the flow
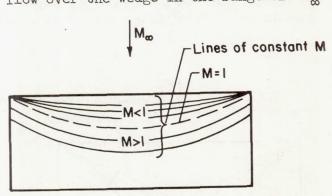will pass through conical-flow

Sketch (a)

---

[3]We ignore the existence of the second - or "strong" - solution in
the present argument, since the wave is assumed attached at the outset.

regions in which the Mach number increases downstream as a result of the relieving effect of the tips. As M_∞ is decreased, the Mach number in the triangular region will decrease toward unity, and the Mach lines from the tip will rotate forward toward the leading edge. Precisely when the Mach number behind the shock wave becomes 1, the triangular region will degenerate into a sonic line coincident with the leading edge. This must occur at the identical value of M_∞ at which sonic speed would be reached on the same wedge in two-dimensional flow. In contrast to the two-dimensional case, however, the local Mach number is not now 1 over the entire wedge but will increase to the rear as a result of the effect of the tips.

Once the flow behind the shock wave has become subsonic, the situation is less certain. In the two-dimensional case (as well as the axially symmetric), the flow is subject to the well-known requirement that the sonic speed must be attained at the shoulder of the wedge (or cone). The arguments leading to this requirement, however (see refs. 3 and 14), depend on properties peculiar to the type of flow in question and do not apply in the present three-dimensional case. All that can be said here is that the sonic line cannot lie downstream of the shoulder. There is nothing that prevents it from occurring upstream of the shoulder on the face of the wedge.

With this fact in mind, a few conjectures can be made concerning the flow over the wedge in the range of M_∞ in which the shock wave is still attached but the flow behind it is subsonic. In view of the sequence of events described for higher values of M_∞, it seems likely that here the situation on the surface of the wedge will be more or less as shown in sketch (b). According to the earlier considerations regarding conditions at the leading edge, this edge will appear as a line of constant subsonic Mach number. The other lines of constant M, including the sonic line, will presumably curve toward the rear somewhat as shown in the sketch.

Sketch (b)

Whether or not these lines will remain anchored to the leading edge of the tip is an open question. The subsonic lines will probably remain so, since the spanwise flow could hardly negotiate the square corner at the tip without becoming supersonic. The sonic line might go to the same point as shown in the sketch or meet the tip at some point aft of the leading edge and then run forward along the square corner. Some or all of the supersonic lines will probably run to the tip aft of the leading edge. In any event, the Mach number at the leading edge will decrease as M_∞ is decreased, and the lines of constant M may be expected to move progressively toward the rear. Eventually the subsonic Mach number corresponding

to shock detachment will appear at the leading edge, and further decrease
in M_∞ will give rise to a detached wave as discussed before.

Once detachment has occurred the situation is still less definite.
It seems likely to the writer that the initial detachment will be only
partial in the sense that the wave will still remain attached at the tips
(which are singular points and therefore not subject to the earlier argu-
ments). While this condition prevails, the detached portions of the wave
will move away from the wedge as M_∞ decreases, though at a probably
slower rate than in the two-dimensional case. Eventually detachment must
occur also at the tips, and the entire wave move forward toward infinity
as M_∞ approaches 1. While all this is going on, the lines of constant
M will continue to move rearward on the wedge as before. The ideas of
this paragraph are, however, purely speculative and cannot be checked from
the present measurements of surface pressure at relatively wide intervals
of M_∞. A detailed investigation of the detachment process for a wedge
of finite span would be of interest.

RESULTS AND DISCUSSION

The results of the investigation are presented in figures 3 through
17. As in reference 11, the Mach number range is from 1.166 to 1.377,
which brackets the attachment value of 1.221 given by exact inviscid
theory for the present section. The range of angle of attack is from
0° to something less than 5°, depending on the wing in question. Because
of the bulk of the data, it is not practicable to give complete pressure-
distribution results for each Mach number and angle of attack. As in
reference 11, however, sufficient data are given to illustrate the observed
phenomena. The values of the free-stream Mach number, though listed to
three decimal places, are considered to be accurate to ±0.004 (see ref.
11). The use of the three-place values in plots with Mach number as the
independent variable is found to give consistently less scatter than is
obtained when they are rounded off to two places. All the data were taken
at approximately the same Reynolds number as in the earlier work (0.54
million based on the airfoil chord).

Characteristics at Zero Angle of Attack

Pressure distribution.- Representative data for the distribution of
pressure at zero angle of attack are given in figures 3 and 4 for $A = 4$
and 2, respectively. In both cases results are shown for two free-stream
Mach numbers, one to each side of the attachment value. To provide a
frame of reference, the chordwise pressure distribution given by the
transonic small-disturbance theory for $A = \infty$ (refs. 2 and 11) has been

reproduced at each of the spanwise stations. Experimental points for
$A = \infty$, taken from the work of reference 11, are included for comparison
at midspan.[4]

A general comparison of parts (a) and (b) of each figure shows a
characteristic difference in the type of pressure distribution that pre-
vails on the front wedge at Mach numbers below and above attachment. This
difference - nonuniform chordwise distribution below attachment, uniform
distribution above - was also observed in the two-dimensional results of
reference 11. It appears here at inboard stations, where the flow at Mach
numbers above attachment is largely uninfluenced by the presence of the
tips (see next paragraph). At outboard stations at Mach numbers below
attachment the effect of the tips is to reduce the chordwise variation of
pressure. Above attachment the opposite is true. As a result the distri-
bution of pressure on the front wedge near the tips is much the same at
the two Mach numbers. On the rear wedge the pressure distribution shows
no essential difference between the two cases.

At Mach numbers above attachment (figs. 3(b) and 4(b)), the influence
of the finite span is confined to a region aft of the Mach line from the
tip of the leading edge. The theoretical location of this line, as cal-
culated from the transonic small-disturbance theory, is shown in the
figures.[5] Ahead of this line the measured pressures on both wings agree
almost exactly with the experimental values obtained for $A = \infty$ (and hence
with the theoretical curves for infinite span; cf. ref. 11, p. 13). This
is, of course, as it should be. Behind the Mach line from the tip, outflow
toward the end of the wing reduces the compression on the front wedge, with
a resulting decrease in C_p. The point at which this decrease begins is
seen to agree well with the calculated location. The outflow that causes
the decrease evidently carries over onto the rear wedge, with the result
that the pressures on this wedge are also lower at most points than those
measured in the two-dimensional case. This is especially true at the
midspan of the $A = 2$ wing, where the effects of both tips are felt simul-
taneously. Within the region influenced by the part of the tip aft of
the ridge line (the boundaries of which cannot yet be calculated), there
is apparently an inflow onto the wing as a result of the substream pres-
sures on the rear wedge. This causes a local increase in pressure toward

---

[4]In contrast to the situation in figure 3 of reference 11, the present
plots show only one set of experimental points at each station. For $A = \infty$
and 2, the data given are those obtained at a zero angular setting
approached from the positive side (see ref. 11, pp. 9 and 12). For $A = 2$
the differences between these data and those obtained at a zero setting
approached from the negative side were of the same order as the corre-
sponding differences shown for $A = \infty$ in reference 11. For $A = 4$ the
data given in figure 3 were read from plots of pressure coefficient versus
angle of attack as previously described.

[5]The calculation requires the use of equation (68) of reference 2
and the results of Appendix C of reference 9.

the tip on both wings. As would be expected, the chordwise pressure dis-
tributions at stations an equal distance in from the tip on the two wings
agree well, at least until the effect of the opposite tip is encountered.
(The slightly lower pressures on the A = 2 wing may be due to differences
in the air stream at the positions at which the tips were located in the
tunnel; cf. ref. 11, pp. 5-6.) We may thus say that in general - and
as would be expected - the tip effects at Mach numbers above attachment
are nearly identical for the two wings. Any differences that appear in
the over-all coefficients must therefore be due to differences in the
percentage of the total wing area enclosed by the Mach lines from the tip.

At Mach numbers below attachment (figs. 3(a) and 4(a)), the flow
downstream of the bow wave is subsonic, and tip effects are evident across
the entire span. On the front wedge the values of C_p are now everywhere
less than those obtained in the two-dimensional case. As surmised in the
earlier discussion, the measured sonic line is curved and lies well forward
of the ridge.[6] The situation on the rear wedge, where the flow is still
supersonic, is much the same as that observed when the shock wave is
attached. In this case, however, the outflow, which is now apparent across
the entire front wedge, carries over to some extent onto the entire rear
wedge (compare the pressure distributions at midspan in figs. 3(a) and
(b)). The inflow from the rear half of the tip is confined, as before,
to a small area adjacent to the tip. There is now, of course, no reason
why the pressure distributions at equal distances in from the tip should
be the same for the two wings. On the contrary, the effects of finite
span are, as might be expected, everywhere larger for the wing of aspect
ratio 2. At the midspan station for A = 4, in fact, the present results
approach closely those obtained for A = ∞.

As in the two-dimensional results of reference 11, viscous effects
are apparent throughout the present data. This is especially true on the
rear wedge. The details are essentially the same as in the earlier work
(see ref. 11, p. 13).

Sonic line.- To examine the changes in the sonic line with aspect
ratio and Mach number, the position of this line has been plotted in
figure 5 for the three subattachment Mach numbers provided in the present
tests. The nearly constant position of the sonic point for A = ∞ (ref.
11) is also shown. It can be seen that at a given M_∞ the sonic line
moves generally forward toward the leading edge as the aspect ratio is
reduced. For a given aspect ratio, the sonic line on the finite wings

---

[6]The location of the sonic line from the measured pressures involves
the assumption that the detached wave is normal to the free stream at all
points directly forward of the leading edge. This is actually the case
only at the midspan plane of symmetry. At the present Mach number, how-
ever, any errors from this source should be within the accuracy of the
experimental data.

moves aft toward the ridge with reduction in Mach number. The latter behavior, which is in contrast to the fixed position observed for infinite span, corroborates the remarks made earlier in the report. It is not clear from the data whether the sonic line ends at the intersection of the tip and the leading edge, though this would appear to be more or less the case in most instances. (The shape of the line near the leading edge is only approximate, since the forwardmost orifice was at 6 percent of the chord.) On the aspect-ratio-4 wing at $M_\infty = 1.166$ it appears that the line might intersect the tip aft of the leading edge as previously conjectured.

Figure 5 suggests that the two- and three-dimensional cases may have a significant difference beyond those already discussed. In the two-dimensional case, the length that fixes the scale of the flow field over the front wedge when a subsonic region exists - indeed the only independent length in the problem - is the chordwise distance c_f from the leading edge to the ridge line. As is well known, the flow in this case is characterized by an interaction between the supersonic expansion fan that originates at the ridge and the subsonic region that surrounds the wedge.[7] This interaction arises from the fact that certain of the Mach waves of the expansion fan bend forward to meet the sonic line, which runs in this case from the ridge to a point on the bow wave. It is to be expected that the same situation will occur, with minor modifications, in the three-dimensional case - that is, expansion waves from the ridge will bend forward to meet the sonic surface, which now runs from the sonic line on the face of the forward wedge to a corresponding line on the shock wave. Under these conditions, the flow field will depend on two lengths, the chord c_f and the span b - or, what is equivalent, the chord c_f and the aspect ratio b/c_f.

Study of figure 5 suggests that yet another situation may exist in the three-dimensional case. In particular, the large distance by which the sonic line lies forward of the ridge for $A = 2$ makes it seem highly unlikely that the expansion from the ridge will in all cases meet the sonic surface before this surface is intercepted (and terminated) by the shock wave. If it does not, then the region ahead of the expansion fan is independent of the chord, and the scale (but not the extent) of this part of the flow must depend only on the span b. Precisely this condition is known to exist on a finite-span wedge when the bow wave is attached and the flow is everywhere supersonic. The present considerations suggest that it will continue to exist at values of M_∞ smaller than that at which a subsonic region first appears in the flow. If this is true, there must be, as the Mach number is reduced, a limiting value of M_∞ at which the entire field first becomes affected by the chord. This value will depend presumably on the aspect ratio b/c_f and the wedge angle θ_W (as well as the ratio of specific heats γ).

---

[7]The flow is, however, independent of conditions aft of the ridge; (see ref. 2, pp. 3-4).

On the assumption that the foregoing situation does in fact exist, something further can be said about the sonic line. According to the transonic similarity rules (see ref. 15, eqs. (31) and (40)), the line at which $M = 1$ on a thin wedge must be given, in general, by an equation of the form

$$\frac{x}{c_f} = f_1 \left\{ \frac{M_\infty^2 - 1}{\left[(\gamma + 1)M_\infty^2 \theta_w\right]^{2/3}} \ , \ \left[(\gamma + 1)M_\infty^2 \theta_w\right]^{1/3} \frac{b}{c_f} \ ; \ \frac{y}{b} \right\} \qquad (1)$$

where f_1 is some function of the three parameters inside the braces. For conditions in which the flow is independent of c_f, this quantity must disappear from the equation. This will happen only if the aspect-ratio parameter enters as a multiplying factor on the right-hand side. Making this change gives finally

$$\frac{x}{b} = \left[(\gamma + 1)M_\infty^2 \theta_w\right]^{1/3} f_2 \left\{ \frac{M_\infty^2 - 1}{\left[(\gamma + 1)M_\infty^2 \theta_w\right]^{2/3}} \ ; \ \frac{y}{b} \right\} \qquad (2)$$

where f_2 is now a function only of the transonic similarity parameter and y/b. An equation of this type will hold for the sonic line on the front wedge as long as the value of M_∞ exceeds that below which the entire flow field becomes affected by the chord. This lower limit would presumably be given in the present approximation by some relationship between the aspect-ratio and transonic similarity parameters of equation (1). An experimental check of equation (2) would be of some interest.

Spanwise drag distribution.- The spanwise distribution of the section pressure-drag coefficient at zero angle of attack is shown in figure 6 for the two Mach numbers considered in figures 3 and 4. Results are given separately for the front wedge, rear wedge, and complete wing.[8] The fairing of the curves to zero at the tip is arbitrary.

The phenomena noted in the pressure distributions are again apparent in figure 6. Consider first the data at $M_\infty = 1.280$. At this Mach number the drag coefficient of the front wedge at midspan is essentially the same for both wings and equal to the corresponding value for the airfoil section in two-dimensional flow. For $A = 4$ this value is maintained out to $y/c = -1$, beyond which the drag begins to fall. For $A = 2$ the drag of the front wedge starts to fall immediately as one moves out along the span. This is in keeping with the results of figures 3(b) and 4(b) regarding the regions influenced by the tip. At this Mach number the curves for the two front wedges are seen to be similar with distance in from the tip, but not

---

[8]The coefficient is referred in each case to the total chord of the wing section.

identical as they theoretically should be. The somewhat lower drag for
A = 2 may be due to differences in the air stream as previously noted.
On the rear wedge at $M_\infty = 1.280$, the drag at midspan for A = 4 is in
agreement with the two-dimensional value, whereas that for A = 2 is
considerably higher. This is a result of the fact that the effect of
the tips of the front wedge extends to the midspan in the one case but
not in the other (cf. figs. 3(b) and 4(b)). For A = 4 the tip effect
is encountered only as one proceeds out along the span, and then the drag
of the rear wedge does rise above its two-dimensional value. Close to
the end of the wing the effect of the tip of the rear wedge causes a
decrease in the drag of this wedge for both aspect ratios. The results
for the complete wing combine the above effects.

At $M_\infty = 1.183$ the drag of the front wedge on both wings is every-
where less than the two-dimensional value. This is due to the fact that
the tips of the front wedge now influence the flow everywhere on the wing.
This influence also causes the drag of the rear wedge to be higher than
the two-dimensional value at all stations, except those in the region
influenced by the tip of the rear wedge itself. As pointed out in con-
nection with figures 3(a) and 4(a), these effects are all more pronounced
on the wing of smaller aspect ratio.

Integrated drag.- Results for the integrated pressure drag at zero
angle of attack are shown as a function of free-stream Mach number in
figure 7. Theoretical results are included here from transonic small-
distrubance theory for A = ∞ and from linear theory for all aspect
ratios. The latter results were obtained from the work of Nielsen (ref.
16).

As would be expected from the previous data, the measured drag coef-
ficient of the front wedge decreases with decreasing aspect ratio at all
values of M_∞. This result is most pronounced at the lower Mach numbers
where the shock wave is detached. The measured drag of the rear wedge
increases with decreasing aspect ratio, the increasing effect of the tips
of the front wedge apparently predominating over the decreasing effect of
the tips of the rear wedge (cf. fig. 6). In contrast to the situation on
the front wedge, the result here is little affected by Mach number. For
both wedges the direction of the variation with aspect ratio is given
correctly by linear theory, but the quantitative predictions are, for the
most part, in considerable error. For the complete wing the data show
the same trends as for the front wedge, though somewhat diminished by
the compensating effects of the rear wedge. Here linear theory shows no
influence of aspect ratio (within the range of variables shown). This
is experimentally the case only at the higher values of M_∞. From the
practical point of view, the main effect of reducing the aspect ratio is
to reduce the rise in drag coefficient as the Mach number decreases into
the transonic range.

It is of interest to compare the present results with those of Orman,
Rae, and Ward for wings of lower span (ref. 12). Because of a difference

in thickness ratio between the two investigations, this is best done in
a transonic similarity plot such as figure 8. (For the theory behind
this type of plot, see ref. 15.) Here results for the complete wing are
shown for two values of the transonic similarity parameter. One of these
(ξ_∞ = 1.26) was chosen to conform exactly to the lowest value of M_∞ used
in reference 12. (This value of ξ_∞ corresponds approximately to the
attainment of sonic flow just behind an attached shock wave.) The data
for the points shown from the present test were taken from curves faired
through the experimental values of figure 7. It is apparent from figure 8
that the results from the present test fall nicely into line with the data
of reference 12. The excellence of the agreement is, in fact, a bit sur-
prising, since the models of reference 12 were of the semispan type and
hence subject to effects of the tunnel-wall boundary layer.

Characteristics at Angle of Attack

Load distribution.- The distribution of normal force per unit angle
of attack is shown in figures 9 and 10 for the Mach numbers considered
in figures 3 and 4. Results are shown in each case for angles of attack
of approximately 1° and 4°. Data for 0.3°, which were included in refer-
ence 11, have been omitted here for simplicity. As in figures 3 and 4,
the chordwise distribution given by two-dimensional transonic theory
(refs. 9 and 11) is reproduced at each spanwise station. These results
are derived on the assumption of a vanishingly small angle of attack.
In the present figures the experimental data from reference 11 are plotted
slightly to the right of the midspan station to avoid confusion.

Before considering these figures it should be mentioned that at
$M_\infty = 1.280$ (figs. 9(b) and 10(b)) the shock wave is still attached to the
leading edge at $\alpha \cong 1^\circ$. According to the measured pressures, the flow
just behind the wave on the lower surface at this angle is slightly super-
sonic for $A = 2$ and 4. For $A = \infty$, however, it is slightly subsonic.
This is due to the somewhat higher actual angle of attack caused by the
greater sting deflection in this last case (cf. ref. 11, p. 8). For
$M_\infty = 1.280$ the shock wave is well detached at $\alpha \cong 4^\circ$. It is, of course,
detached at all angles of attack for $M_\infty = 1.183$.

As would be expected, the general effect of finite span is to decrease
the loading toward the tips. The manner in which this takes place varies
somewhat with M_∞, A, and α. In the following discussion of the details
most of the remarks will be concerned with conditions on the front wedge.
Since this half of the wing carries the majority of the load at the Mach
numbers considered, such emphasis is reasonable.

As between the two Mach numbers (parts (a) and (b) of each figure),
the situation at $\alpha \cong 1^\circ$ on the front wedge is much the same as that
already observed at $\alpha = 0^\circ$. At inboard stations, where the tip effects
are unimportant at the higher Mach number, there is again a characteristic

difference of the type found in the two-dimensional case (i.e., uniform load at the higher Mach number, nonuniform at the lower). The difference appears here, however, over less of the wedge than at $\alpha = 0°$. This is a result of an increase in the region of influence of the tip with angle of attack at the higher Mach number. At outboard stations at $\alpha \cong 1°$ the chordwise distribution of load is similar (i.e., nonuniform) at both Mach numbers. At $\alpha \cong 4°$, where the shock wave is detached at both values of M_∞, the latter situation prevails at all stations.

As to a comparison of the two aspect ratios at a given Mach number, no extended discussion like that for $\alpha = 0°$ will be attempted here. Suffice it to say that at a given α the local loading at a given station in from the tip is less for aspect ratio 2 than 4. This is as would be expected except for $\alpha \cong 1°$ at $M_\infty = 1.280$. In this case the loading should be the same on both wings in those regions that are influenced by only one tip. The fact that they are somewhat different is most likely due to the relative unreliability of the angle of attack for $A = 4$ as mentioned on page 6.

A comparison of the data at the two angles of attack for a given A and M_∞ shows that, generally speaking, the loading per unit angle on the front wedge decreases as the angle increases. This same result was noted previously in the two-dimensional data of reference 11. Reduction in aspect ratio tends, however, to reduce this effect, especially near the tips where the dependence on α disappears almost entirely. For aspect ratio 2, in fact, the influence of α is quite small over the entire wedge. It follows from this that the results of lift coefficient versus angle of attack should exhibit an increasing linearity as the aspect ratio is reduced.

As in the two-dimensional case (see ref. 11, p. 15), the distribution of load on the rear wedge is critically influenced by viscosity. In the former work, interaction of the boundary layer and the trailing shock wave was found to cause a reduction in loading over the rear portion of the chord at the lower angles of attack. The same effect is visible to a varying degree in figures 9 and 10. In most cases the result is here less pronounced than in the two-dimensional data. It has, in fact, largely disappeared on the wing of aspect ratio 2 at $M_\infty = 1.183$. On the same wing at $M_\infty = 1.280$, however, the effect is intensified. As a result the region of negative lift, which was noted in the two-dimensional data at $\alpha \cong 0.3°$, persists here up to $\alpha \cong 1°$. The reasons for this entire behavior are not clear. As in the two-dimensional case, it is to be expected that the viscous effects would be reduced by an increase in Reynolds number above the present low value of 0.54 million.

Spanwise lift distribution.- The spanwise distribution of section lift coefficient per unit angle of attack is shown in figure 11 for the cases covered in figures 9 and 10. The results call for little comment in view of the foregoing discussion. On the front wedge for $A = 4$, $\alpha \cong 1°$, and $M_\infty = 1.280$, the lift coefficient at midspan lies above the

two-dimensional value. This unlikely result is probably due again to the
unreliability of the angle of attack for this wing. On the rear wedge at
M_∞ = 1.280, the spanwise distribution on both wings at $\alpha \cong 1^\circ$ shows a
local increase just inboard of the tip. This effect is not present at
the lower Mach number. The reasons for this behavior, which is probably
attributable to viscosity, are again not clear.

   Integrated lift.- The integrated values of the lift coefficient as
a function of angle of attack are shown in figure 12 for the Mach numbers
at which results were obtained for all wings. Data for the front wedge
are given in figure 12(a) and for the complete wing in figure 12(b). In
both cases results from two-dimensional transonic theory for $\alpha \rightarrow 0$
(refs. 9 and 11) are shown by straight lines terminated arbitrarily at
$\alpha = 3\text{-}1/2^\circ$. The results of this figure are summarized in figure 13, where
lift coefficient per unit angle of attack is plotted as a function of free-
stream Mach number. Data are given for $\alpha \cong 1^\circ$ in figure 13(a) and for
$\alpha \cong 4^\circ$ in figure 13(b). The curves shown here for linear theory were
calculated from the well-known formulas for the lift of a rectangular wing
(see, e.g., ref. 17).

   It is apparent from figures 12 and 13 that the effect of aspect ratio
on the lift increases markedly as the Mach number decreases toward and
past the value for shock detachment. It is clear from figure 13 that
this increase is attributable largely to the front wedge. As in the case
of the drag at zero lift (cf. fig. 7), the effect of aspect ratio on the
rear wedge shows little change with Mach number. What change there is is
confined to the smaller angle of attack where the viscous effects are
large.

   As anticipated from the load-distribution data, reducing the aspect
ratio reduces the nonlinearity that is characteristic of the two-
dimensional results at Mach numbers near shock detachment (cf. ref. 11,
p. 17). This is apparent in both figures 12 and 13. As a result of this
effect, the local increase of lift effectiveness as a function of Mach
number, which characterized the two-dimensional data at low angles of
attack (see fig. 13(a)), is almost completely gone for aspect ratio 2.
The discovery of this increase was one of the interesting results of the
theoretical and experimental work of references 8 to 11. The present data
indicate that the phenomenon is more or less a special characteristic of
two-dimensional flow.

   In figure 13, as in the earlier figure 7, the curves of linear theory
show the correct trend with aspect ratio. Again, however, the values them-
selves are considerably off. For the complete wing, theory and experiment
do appear to agree in several cases. Even in these cases, however, the
agreement is the result of compensating errors on the front and rear
wedges.

   Figure 14 compares the lift results for the present wings with the
data given by Orman, Rae, and Ward in reference 12. The details here are

the same as in the similarity plot of figure 8. As required by the transonic similarity rules (e.g., ref. 15), the experimental points are taken at a constant value of $\alpha/(t/c)$. The value in this instance is fixed by the angle of attack (1°) and thickness ratio (0.0787) of the present data. The curves for linear theory are obtained by expressing the usual formulas (e.g., ref. 17) in terms of the transonic similarity variables. As in figure 8 the experimental data of the present tests fall satisfactorily into line with the results of reference 12.

Center of lift.- The experimental position of the center of lift is shown in figure 15 for the front and rear wedges and for the complete wing. In all cases the location is measured aft from the leading edge of the wing. The data here show more scatter than in previous figures because of inaccuracies inherent in locating the center of lift on the basis of measured pressure distributions. This is especially true at the lower angle of attack, particularly on the rear wedge. The curves for linear theory were calculated again from the usual formulas for a rectangular wing. In general, the effect of reducing the aspect ratio is to shift the measured center of lift forward at all Mach numbers. This is as would be expected and agrees with the trend given by linear theory.

Drag due to angle of attack.- Data on the increase of pressure drag with angle of attack are shown in figure 16 for the various Mach numbers. The results, particularly those for the front wedge (fig. 16(a)), are at first glance rather surprising. In view of the previous data for the lift coefficient (fig. 12(a)), one might expect the present data for the front wedge to show a considerable effect of aspect ratio at Mach numbers below shock detachment. In particular one might expect that, other things being equal, the decrease in lift with decrease in aspect ratio at a given angle of attack would be accompanied by a corresponding decrease in drag due to angle of attack. Instead, the data at Mach numbers below detachment (see fig. 16(a), $M_\infty = 1.166$ to 1.201) show little effect of aspect ratio. Apparently "other things" are not equal.

From resolution of the forces acting on a wing, it can be shown that for small values of α the drag due to angle of attack is given by

$$C_D - (C_D)_0 \cong C_L\alpha + \left[C_C - (C_C)_0\right] \tag{3a}$$

where C_C is the chord-force coefficient and the other symbols have their previous meaning.[9] The first term on the right represents the contribution of the normal force; the second takes account of any change in chord force with angle of attack. Since the data to be examined are not at precisely

---

[9] It is assumed in deriving this equation that C_C is of an order smaller than C_L.

the same α, equation (3a) is divided through by α^2 to obtain

$$\frac{C_D - (C_D)_o}{\alpha^2} \cong \frac{C_L}{\alpha} + \frac{C_C - (C_C)_o}{\alpha^2} \tag{3b}$$

Values for the three terms in this equation, each obtained directly from the experimental data, are shown in figure 17 for the front wedge at $\alpha \cong 4^\circ$.

It can be seen from this figure that for $A = \infty$ the value of $\left[c_{C_f} - (c_{C_f})_o \right]/\alpha^2$ changes from positive to negative as the Mach number decreases past the detachment value. The existence of positive values above detachment can be explained on the basis of the known results for the pressure changes across the leading-edge shock (see, e.g., chart 3 of ref. 18). These positive values would be expected to decrease toward zero as M_∞ increases. The negative values below detachment are associated with the upflow that occurs in the subsonic region between the detached wave and the airfoil. As a result of this upflow, the average pressure on the wedge at angle of attack is less than at zero angle, with a consequent reduction in chord force. This result has already been noted in the pressure distributions of reference 11.

According to figure 17, the effect of reducing the aspect ratio is to reduce the magnitude of $\left[c_{C_f} - (c_{C_f})_o \right]/\alpha^2$ both above and below detachment. The decrease in magnitude of the negative values below detachment is due to the effect of finite span in reducing the size of the subsonic region ahead of the wing (see PRELIMINARY REMARKS). Such a reduction would be expected to decrease the intensity of the upflow and hence to lessen its effect in reducing the average pressure over the wedge. An analogous circumstance may explain the decrease in the positive values of $\left[c_{C_f} - (c_{C_f})_o \right]/\alpha^2$ above detachment. Here the finite span acts to reduce the size of the constant Mach number region on the wedge (see sketch (a), p. 7) and hence to reduce the area in which the pressures are fixed purely by the properties of the leading-edge shock wave. Whatever the explanation, the resulting behavior of the chord force leads to a variation of drag due to angle of attack quite different from that which would be expected on the basis of the normal force alone. In particular, the effect of aspect ratio is greatest at Mach numbers just above detachment and diminishes as the Mach number changes in either direction.

CONCLUSIONS

The principal results of the investigation can be summarized as follows:

1. Flow field: Theoretical considerations indicate that detachment of the shock wave from a wedge of finite span will occur at the same free-stream Mach number as from a wedge of infinite span. The detachment must occur simultaneously at all points across the span (except possibly the tips). At Mach numbers below detachment the sonic speed at zero angle of attack need not be attained at the ridge as in the two-dimensional case but may occur forward on the face of the wedge. This fact is confirmed by experiment. For a range of Mach number below detachment it seems likely that the flow field near the leading edge will be independent of the chord of the wedge. Under these conditions the governing (and only) characteristic length in the problem is the span.

2. Drag at zero lift: The pressure drag coefficient at zero lift decreases with decreasing aspect ratio at all values of the free-stream Mach number. This effect is most pronounced at the lower Mach numbers where the shock wave is detached. As a result, the rise in drag coefficient with decreasing Mach number, which was found in the two-dimensional case, becomes less pronounced as the aspect ratio is reduced.

3. Lift: Decreasing the aspect ratio decreases the rise of lift with angle of attack. This effect grows rapidly as the shock wave becomes detached. Decreasing the aspect ratio also decreases the nonlinearity of the lift curve at Mach numbers near shock detachment. Because of this, the local peak of initial lift-curve slope as a function of Mach number, evident in this vicinity in the two-dimensional case, is almost completely gone at aspect ratio 2.

4. Drag due to angle of attack: The drag due to angle of attack is affected by a variation of chord force as well as normal force. On the front wedge in the two-dimensional case, the increment in chord force (as measured from the chord force at zero angle) changes from positive to negative as the shock wave detaches. Reducing the aspect ratio reduces the magnitude of this change. The result, when this variation is combined with that of the normal force, is that the effect of aspect ratio is greatest at Mach numbers just above detachment and diminishes as the Mach number is changed in either direction.

Ames Aeronautical Laboratory
    National Advisory Committee for Aeronautics
        Moffett Field, Calif., June 29, 1955

REFERENCES

1. Guderley, K. Gottfried: Considerations of the Structure of Mixed Subsonic-Supersonic Flow Patterns. Tech. Rep. No. F-TR-2168-ND, AAF, Air Materiel Command (Wright Field), Oct. 1947.

2. Vincenti, Walter G., and Wagoner, Cleo B.: Transonic Flow Past a Wedge Profile With Detached Bow Wave. NACA Rep. 1095, 1952. (Supersedes NACA TN's 2339 and 2588.)

3. Liepmann, H. W., and Bryson, A. E., Jr.: Transonic Flow Past Wedge Sections. Jour. Aero. Sci., vol. 17, no. 12, Dec. 1950, pp. 745-755.

4. Bryson, Arthur Earl, Jr.: An Experimental Investigation of Transonic Flow Past Two-Dimensional Wedge and Circular-Arc Sections Using a Mach-Zehnder Interferometer. NACA Rep. 1094, 1952. (Supersedes NACA TN 2560.)

5. Griffith, Wayland: Shock-Tube Studies of Transonic Flow Over Wedge Profiles. Jour. Aero. Sci., vol. 19, no. 4, Apr. 1952, pp. 249-257.

6. Spreiter, John R.: On Alternative Forms for the Basic Equations of Transonic Flow Theory. Jour. Aero. Sci., vol. 21, no. 1, Jan. 1954, pp. 70-72.

7. Spreiter, John R.: Errata on Alternative Forms for the Basic Equations of Transonic Flow Theory. Jour. Aero. Sci., vol. 21, no. 5, May 1954, p. 360.

8. Guderley, Gottfried, and Yoshihara, Hideo: Two-Dimensional Unsymmetric Flow Patterns at Mach Number 1. Jour. Aero. Sci. vol. 20, no. 11, Nov. 1953, pp. 757-768.

9. Vincenti, Walter G., and Wagoner, Cleo B.: Theoretical Study of the Transonic Lift of a Double-Wedge Profile With Detached Bow Wave. NACA Rep. 1180, 1954. (Supersedes NACA TN 2832.)

10. Yoshihara, Hideo: On the Flow Over a Wedge in the Upper Transonic Region. WADC Tech. Rep. 53-478, U. S. Air Force, Nov. 1953.

11. Vincenti, Walter G., Dugan, Duane W., and Phelps, E. Ray: An Experimental Study of the Lift and Pressure Distribution on a Double-Wedge Profile at Mach Numbers Near Shock Attachment. NACA TN 3225, 1954.

12. Orman, P. L., Rae, R. S., and Ward, G. N.: Wind Tunnel Test of a Wing of Finite Aspect Ratio of Symmetrical Double Wedge Section at Supersonic Speeds. Proc. Roy. Soc. London, ser. A, vol. 209, no. 1098, Nov. 1951, pp. 309-324.

13. Hilton, John H., Jr.: Flow Characteristics Over a Lifting Wedge of
    Finite Aspect Ratio With Attached and Detached Shock Waves at a
    Mach Number of 1.40. NACA TN 2712, 1952.

14. Busemann, Adolf: A Review of Analytical Methods for the Treatment
    of Flows With Detached Shocks. NACA TN 1858, 1949.

15. Spreiter, John R.: On the Application of Transonic Similarity Rules
    to Wings of Finite Span. NACA Rep. 1153, 1953. (Supersedes NACA
    TN 2726.)

16. Nielsen, Jack N.: Effect of Aspect Ratio and Taper on the Pressure
    Drag at Supersonic Speeds of Unswept Wings at Zero Lift. NACA TN
    1487, 1947.

17. Ferri, Antonio: Elements of Aerodynamics of Supersonic Flows.
    Macmillan Co., N. Y., 1949, pp. 380-381.

18. Staff of the Ames Aeronautical Laboratory: Equations, Tables, and
    Charts for Compressible Flow. NACA Rep. 1135, 1953. (Supersedes
    NACA TN 1428.)
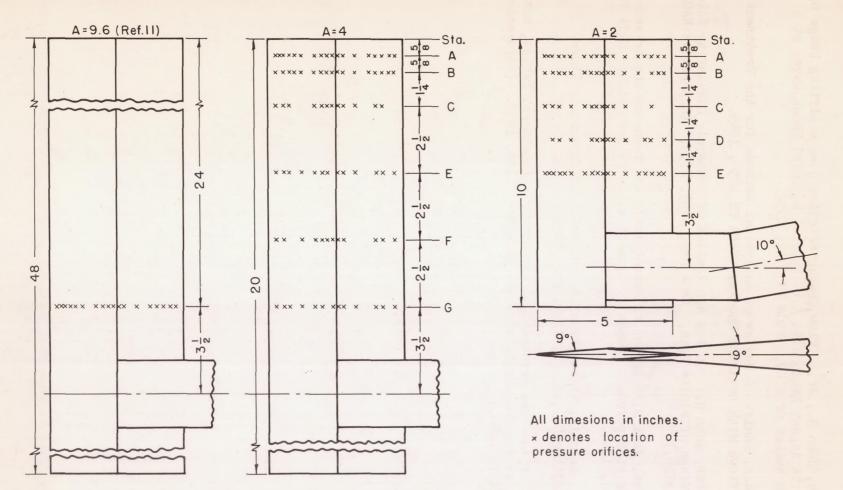
Figure 1.- Dimensions of models.
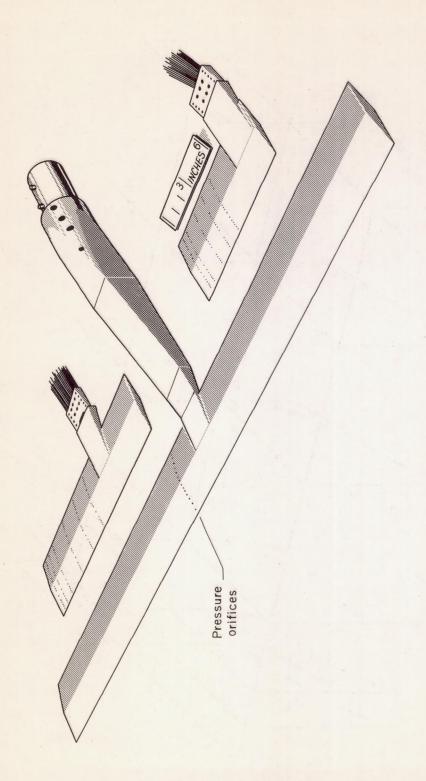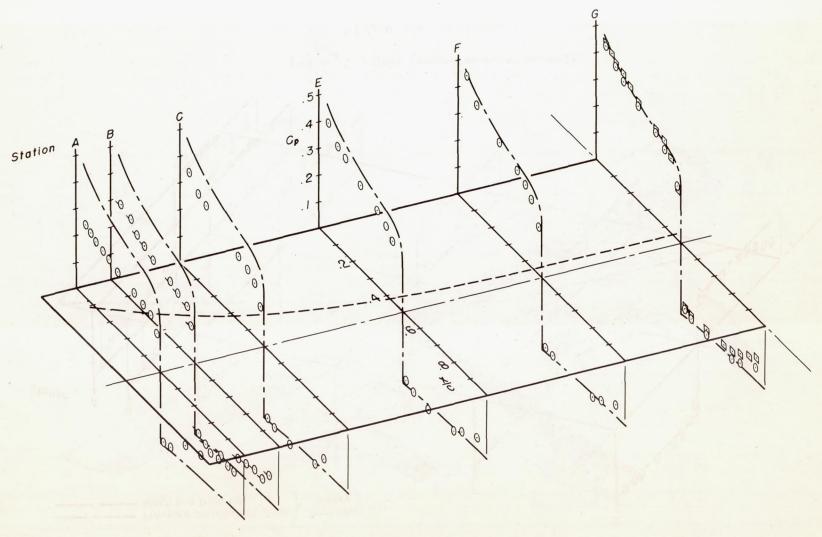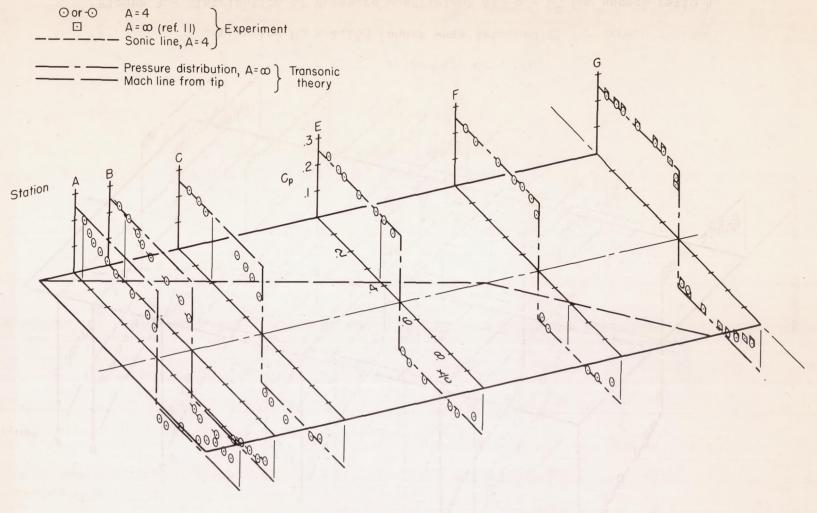
Figure 2.- Sketch of models.
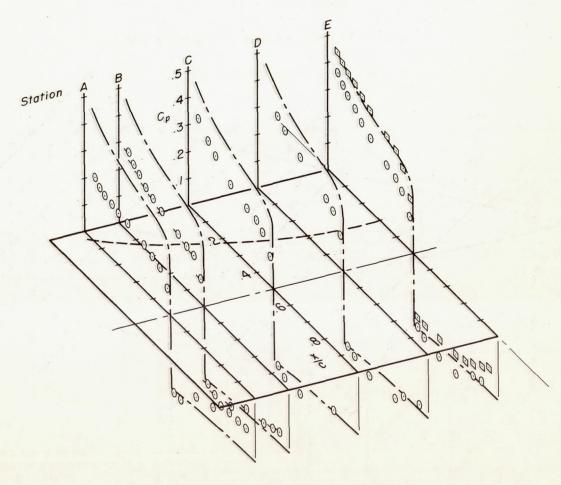
(a) $M_\infty = 1.183$ (shock wave detached).

Figure 3.- Distribution of pressure coefficient at $\alpha = 0^\circ$ for aspect ratio 4.
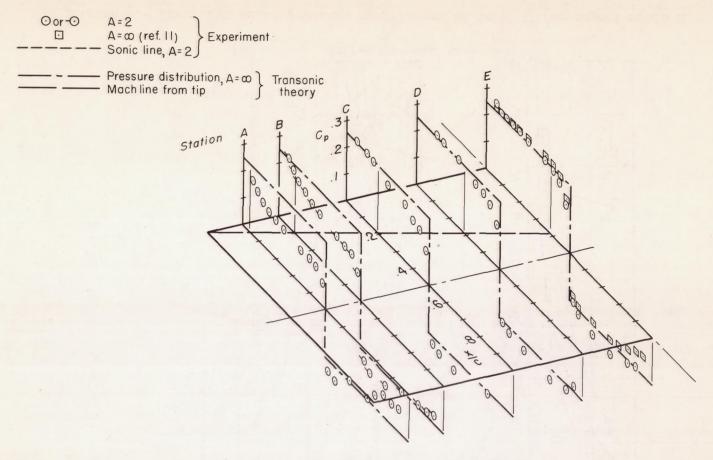
(b) $M_\infty = 1.280$ (shock wave attached).

Figure 3.- Concluded.

(a) $M_\infty = 1.183$ (shock wave detached).
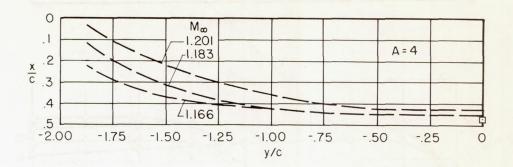
Figure 4.- Distribution of pressure coefficient at $\alpha = 0^O$ for aspect ratio 2.

Legend:

⊙ or ⊖ A = 2
□ A = ∞ (ref. 11) } Experiment
— — — — — Sonic line, A = 2

— · · — Pressure distribution, A = ∞ } Transonic
— — · · — Mach line from tip } theory

(b) $M_\infty = 1.280$ (shock wave attached).

Figure 4.- Concluded.
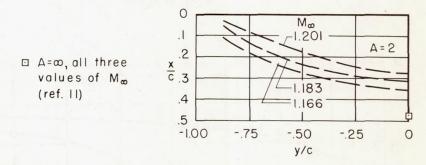
Figure 5.- Position of sonic line on surface of wing at $\alpha = 0^\circ$.
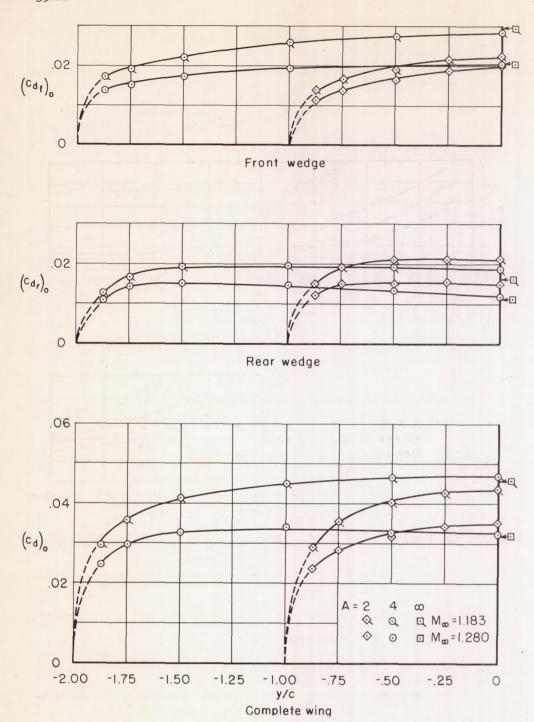
Figure 6.- Spanwise distribution of section drag coefficient at $\alpha = 0^{\circ}$.
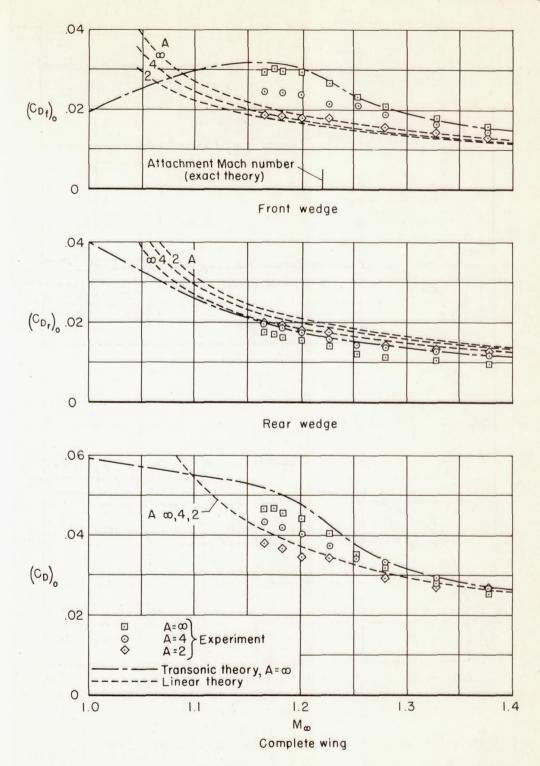
Figure 7.- Pressure-drag coefficient as a function of free-stream Mach number at $\alpha = 0°$.
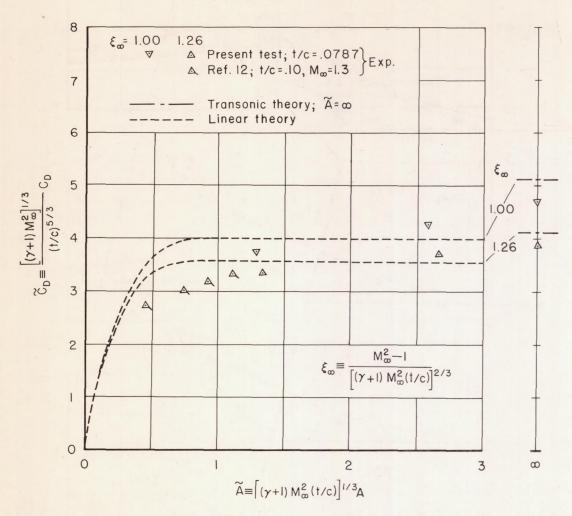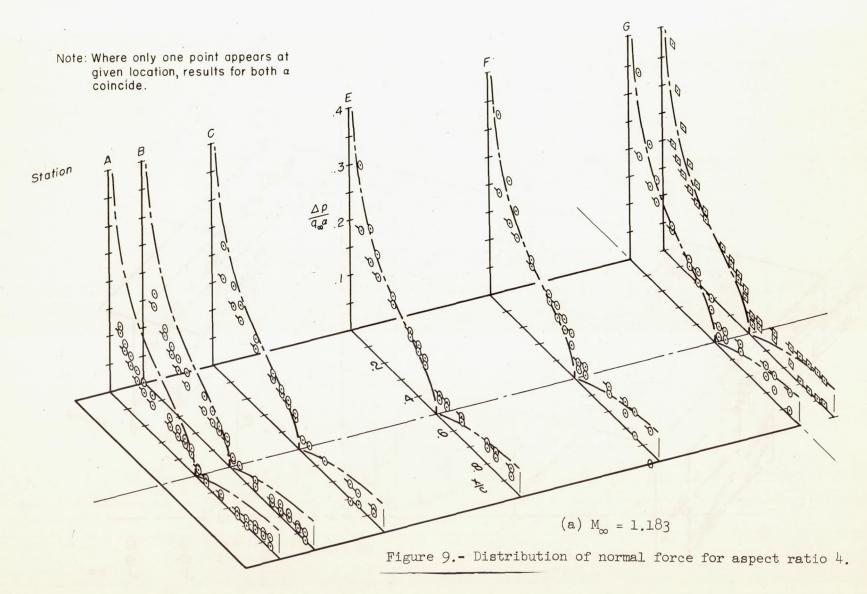
Figure 8.- Pressure-drag coefficient of complete wing at $\alpha = 0^{\circ}$ plotted in transonic similarity form.

Note: Where only one point appears at given location, results for both α coincide.

Station

$\dfrac{\Delta p}{q_\infty a}$

(a) $M_\infty = 1.183$

Figure 9.- Distribution of normal force for aspect ratio 4.

(b) $M_\infty = 1.280$

Figure 9.- Concluded.

Note: Where only one point appears at given location, results for both α coincide.

(a) $M_\infty = 1.183$
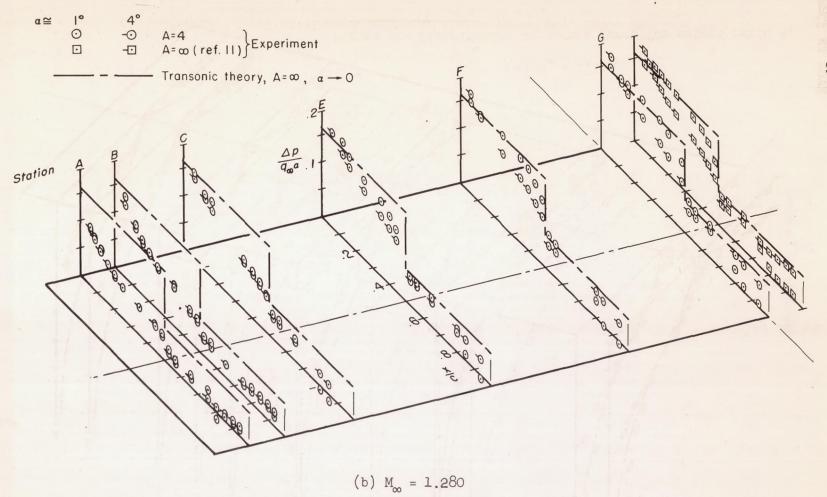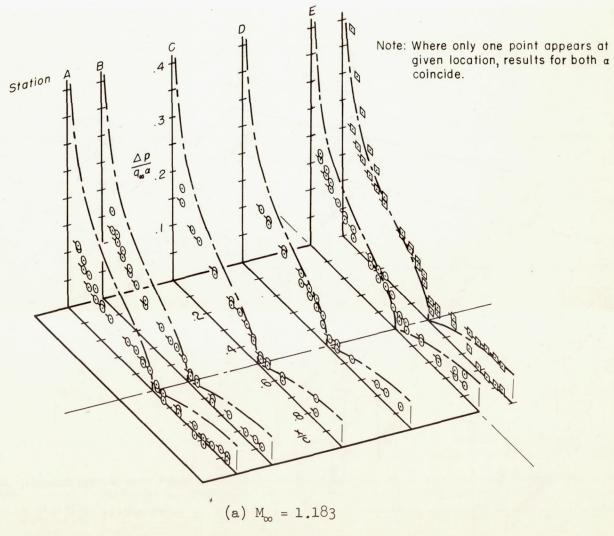
Figure 10.- Distribution of normal force for aspect ratio 2.

(b) $M_\infty = 1.280$
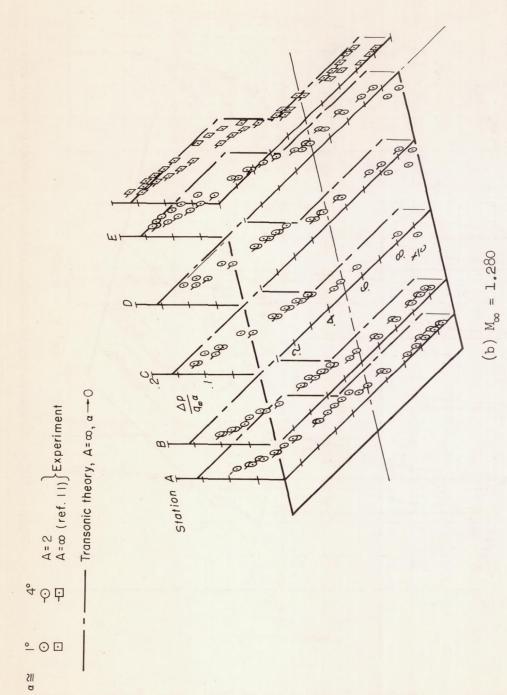
Figure 10.- Concluded.

(a) $M_\infty = 1.183$
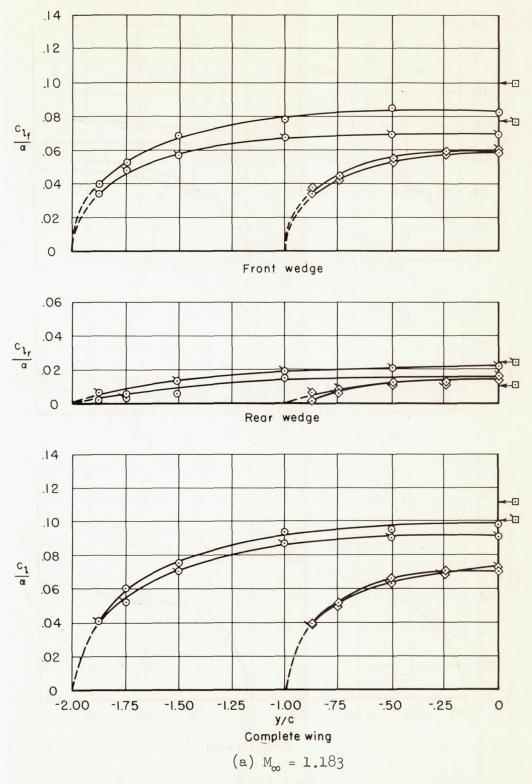
Figure 11.- Spanwise distribution of section lift coefficient.

(b) $M_\infty = 1.280$
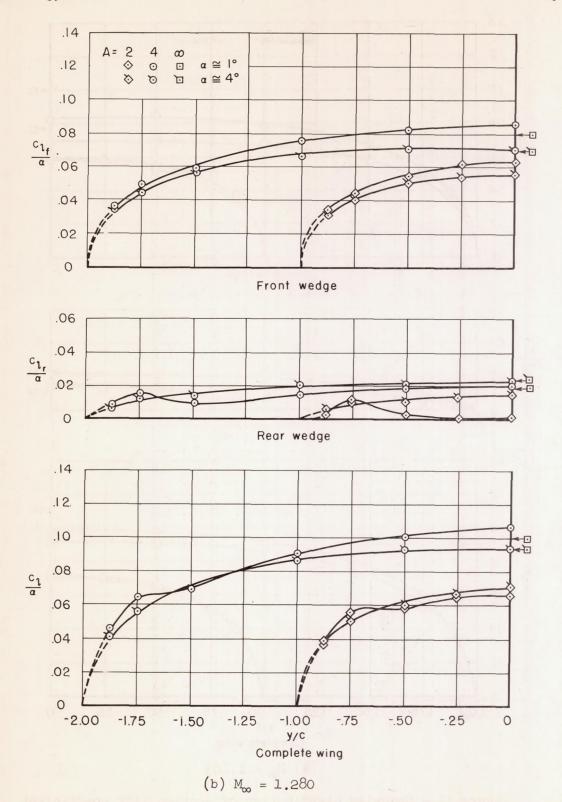
Figure 11.- Concluded.

(a) Front wedge.
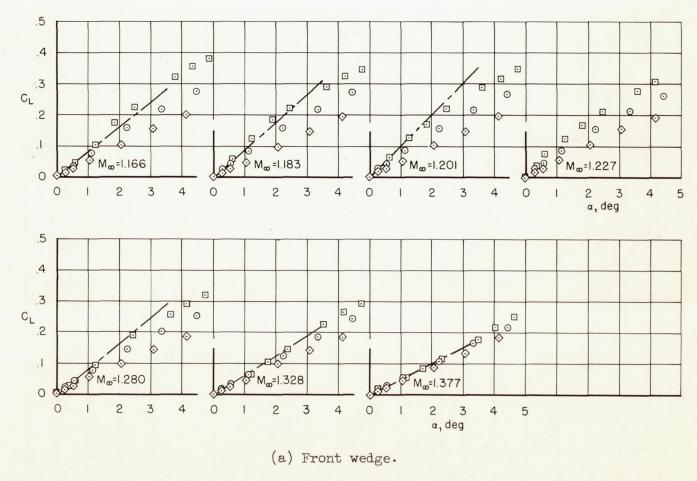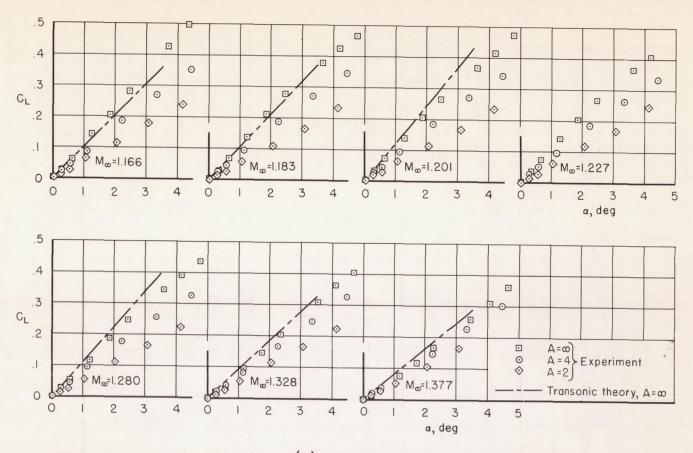
Figure 12.- Lift coefficient as a function of angle of attack for all test Mach numbers.

(b) Complete wing.

Figure 12.- Concluded.

(a) $\alpha \cong 1^{\circ}$
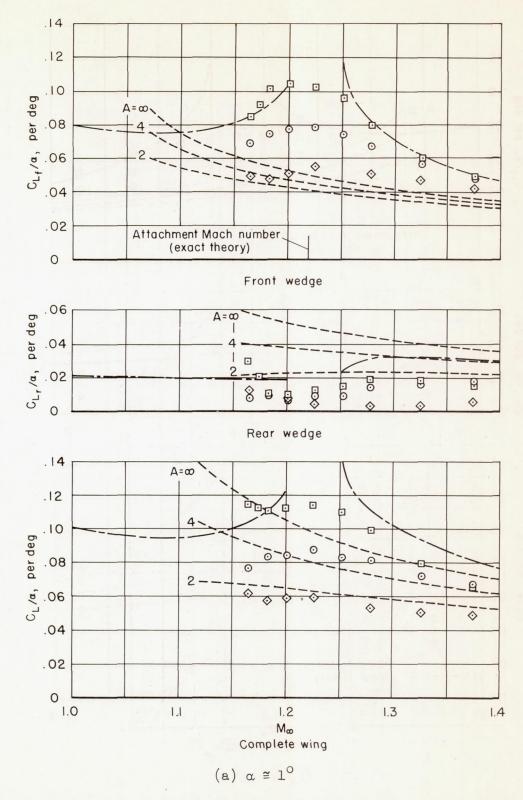
Figure 13.- Lift coefficient per unit angle of attack as a function of free-stream Mach number.

Front wedge

Rear wedge

Complete wing

(b) $\alpha \cong 4^{\circ}$
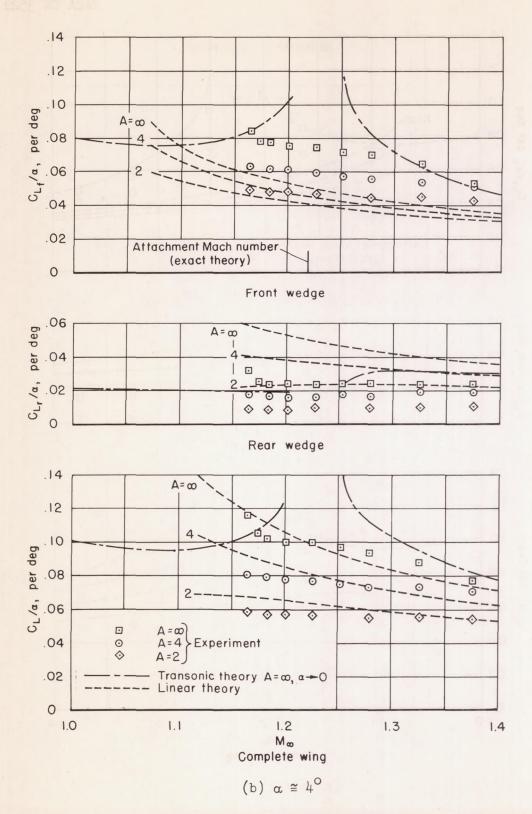
Figure 13.- Concluded.
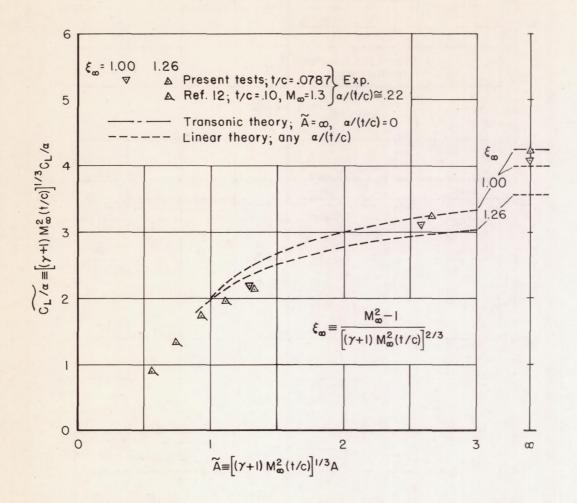
Figure 14.- Lift coefficient per unit angle of attack of complete wing
at $\alpha \cong 1^{\circ}$ plotted in transonic similarity form.

Front wedge

Rear wedge

Complete wing

(a) $\alpha \cong 1°$
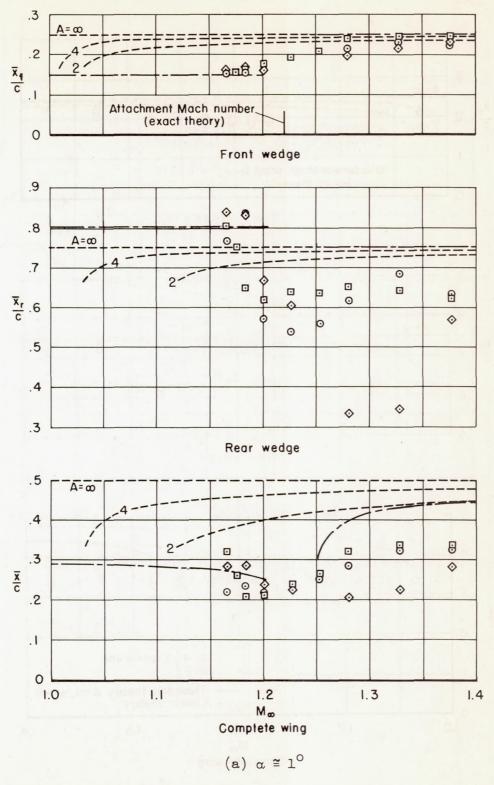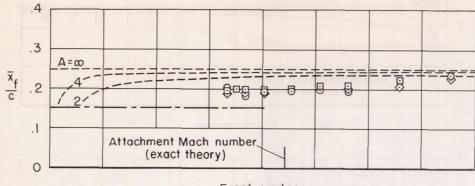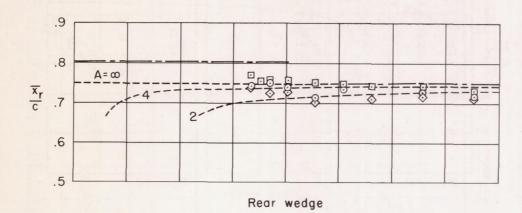
Figure 15.- Chordwise position of center of lift as a function of
free-stream Mach number.
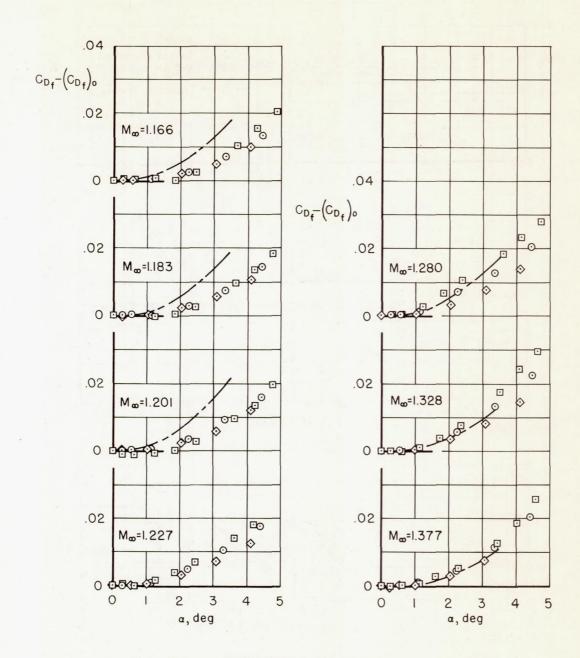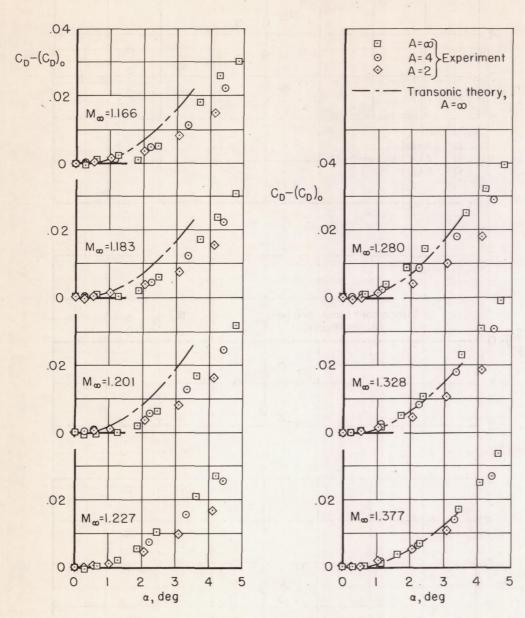
Front wedge

Rear wedge

Complete wing

(b) α ≅ 4°

Figure 15.- Concluded.

(a) Front wedge.

Figure 16.- Increase of pressure-drag coefficient with angle of attack
for all test Mach numbers.

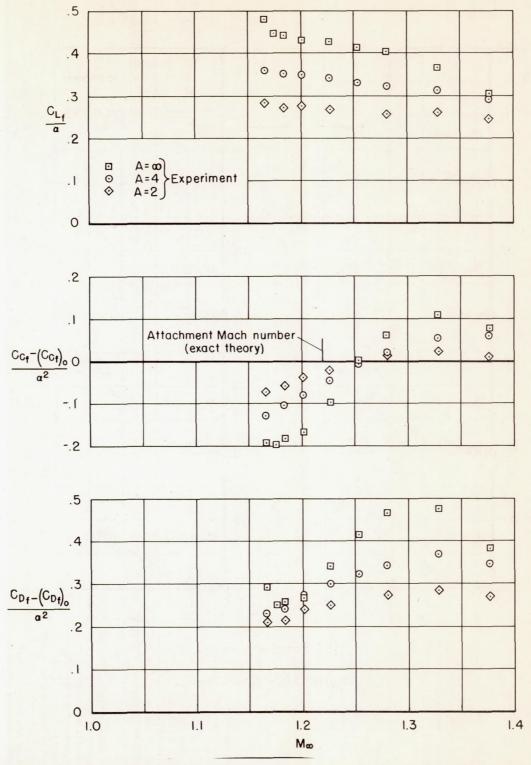(b) Complete wing.

Figure 16.- Concluded.

Figure 17.- Breakdown of drag due to angle of attack for front wedge at $\alpha \cong 4^{\circ}$.